

POWER LOSS REDUCTION IN CENTRIFUGAL PUMP USING SOLID CLEARANCE RING

^{1,2}Dokiparti Satish*,³Ashish Doshi and⁴Mukund Bade

¹Research Scholar, Department of Mechanical Engineering, Sardar Vallabhbhai National Institute of Technology, Surat 395007, Gujarat, India;

²Assistant Professor, Department of Mechanical Engineering, Sarvajani College of Engineering and Technology, Surat 395001, Gujarat, India;

³Assistant Professor, Department of Mechanical Engineering, Sardar Vallabhbhai National Institute of Technology, Surat 395007, Gujarat, India;

⁴Associate Professor, Department of Mechanical Engineering, Sardar Vallabhbhai National Institute of Technology, Surat 395007, Gujarat, India.

*Corresponding author Email: dsatish.3@gmail.com, satish.dokiparti@scet.ac.in

Abstract

Each In the industrial division, the centrifugal pumps consumed most of the energy in motor driven systems for transferring fluid. Electricity consumed by the centrifugal pump is one the major factor contributing the worldwide Carbon Dioxide (CO₂) emission and global warming. This research primarily focuses on reducing the power losses in centrifugal pump, specific speed (N_s) 54 rpm, to improve the efficiency. The power loss due to disk friction losses occurring between back cover plate and impeller back shroud in centrifugal pump was reduced by attaching a solid clearance ring (SCR) on the back cover plate. The experimental analyses were conducted for with and without SCR at rated 1450 and 1000 rpm across the operating flow range. Results showed notable performance improvements: at 1450 rpm, the pump achieved an increase in overall efficiency of 1.74%, while at 1000 rpm, the improvement was 1.56% respectively. For the better understanding of performance enhancement, theoretical head loss variation was also evaluated. In addition, empirical relations on disk friction coefficient (C_m) and power loss due to disk friction (P_{RR}) by various researchers further validated these findings.

Key Words- Centrifugal Pump, Disk Friction Loss, Clearance, Solid Clearance Ring, Power Loss.

1. Introduction

Motor driven system are the major electricity customer in industries at global level generating approximate 6 GT carbon dioxide (CO₂) emissions as per International Energy Agency report [1]. Among the all-motor driven systems, centrifugal pumps consume large part of the energy [2,3]. Because of intrinsic inefficiencies in the pumps, the power that the centrifugal pumps provide to the fluid is always less than the power supplied to it. Internal losses include hydraulic, volumetric, and disk friction losses (DF_l); external losses are mostly mechanical losses brought on by friction in bearings and shaft seals. Among the all losses; DF_l can be countered easily with simple modifications to existing design. It is developed in the clearance (S) between the back shroud of impeller and back cover plate in volute, due to the fluid recirculation in the non-flow zone as shown in Fig. 1 (a). Therefore, lowering the DF_l and increasing pumps overall efficiency (η) can be a workable plan to manage the industrial sector's energy issue and lower CO₂

emissions [4]. It is estimated that, even a 1% enhancement in pump performance can alone reduce the CO₂ emissions about 600 tons per day in European countries [5]. The effective method to reduce this DF_l is to reduce the S on backside by adding the solid clearance ring (SCR) which is termed as back cavity filling. As shown in Fig. 1 (b), the SCR will restrict the recirculation of fluid in S .

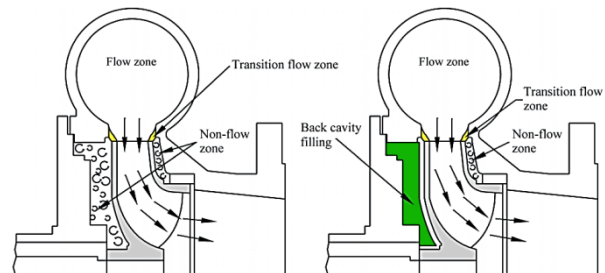


Fig 1. Centrifugal pump (a) without SCR (b) with SCR[6]

Most research communities place emphasis on improving centrifugal pump performance by concentrating on the main flow zone of the pump,

which creates the original flow path and enhances pump performance [7], [8], [9], [10], [11], [12], [13], [14], [15], [16]. Although reduction in S using SCR is rarely researched in literature. Ayad et al. [17] investigated the effect of reducing S on specific speed (N_s) - 28.7 rpm pump performance using numerical analysis. Results reveal that reducing 3 mm S can enhance the head (H) from 3.15 m to 5.9 m and η from 40% to 47%. Cao et al. [18] simulated the effects of varying S by 0.20 mm N_s - 45.2 rpm and found that for each increment of 0.20 mm in S , η reduces by 4.67%. The other simulation done by Pehlivan and Parlak[19] to study the effect of S , wear ring and balancing holes on centrifugal pump with N_s - 22.6 rpm. Compared to the 51.5% η at 40 mm S , the rise in η of 46.2% was obtained at 5 mm S . Kim et al. [20] using water as well as various viscosity crude oils for varying S from 0.25 to 1.00 mm. Volumetric loss decreases with smaller S , dropping from 0.0023 kg/s at 1 mm to 0.0015 kg/s at 0.25 mm for viscous fluids. To assess DF_I and internal flow of the clearance flow channel, Maeda et al. [21] numerically investigated the clearance flow channel, which replicates the clearance flow on the rear of the centrifugal impeller by utilizing rotating disks in a closed chamber. Results showed that the fin reduced DF_I by separating the clearance flow and increasing circumferential velocity. In this research work, an experiential analysis was done on N_s - 54 rpm centrifugal pump to evaluate the pump performance without SCR and with SCR at 1450 rpm and 1000 rpm. The experiments were performed over a wide range of flow rate (Q) to assess the practical feasibility of the SCR. Section 1 in article represents the fundamentals of DF_I and SCR along with the related literature available. Section 2 provides insights of the selected centrifugal pump and overview of whole test setup facility. Section 3 highlights the results obtained from the experiments and theoretical base of it with broad discussion. In the end, Section 4 concludes the major outcomes of this research work.

2. Centrifugal Pump and Experimental Test Setup

As shown in Figure 2, a centrifugal pump, N_s - 54 rpm is analyzed in this experimental work. The pump has design speed (N) of 1450 rpm, H of 5.3 m and Q of 16.81 lps. The inlet (D_i) and outlet diameter (D_o) of pipe is 95.4 mm and 141 mm with impeller width of 30 mm. Pump has 6 curved blades with maximum H and η of 6.2 m and 83%. The clearance (S) between back cover plate and impeller is 13 mm without SCR. The stainless steel (SS) made SCR is used to reduce this available clearance to 1 mm by attaching SCR to back cover plate, as illustrated in Figure 3. The pump

without SCR and with SCR is shown in Figure 4 (a) and (b) respectively.



Fig 2. Actual photograph of the pump, N_s - 54 rpm

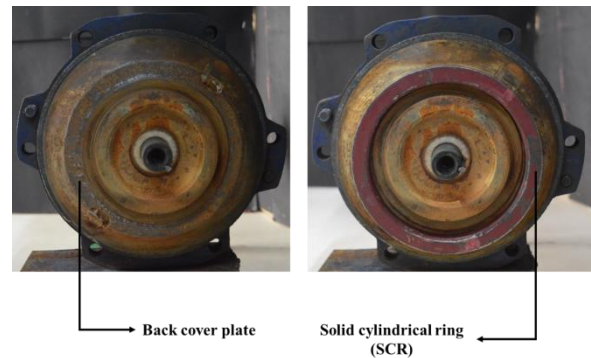


Fig 3. Attachment of SCR on back cover plate.

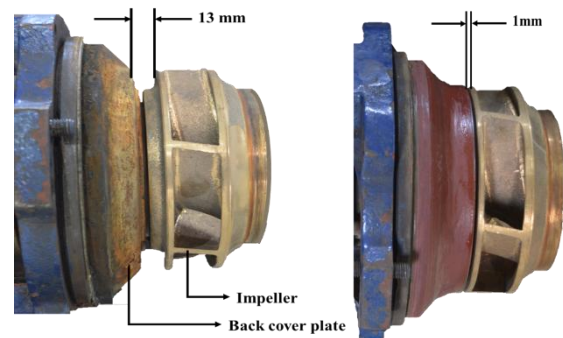


Fig 4. N_s - 54 rpm centrifugal pump (a) without SCR (b) with SCR.

To experiment the selected pump, the well-established and calibrated test setup at Fluid Mechanics and Fluid Machine Laboratory, SardarVallabhbbhai National Institute of Technology, Surat, Gujarat, India was used. The schematic of test setup is shown in Figure 5 with actual experimental test setup in Figure 6. This open loop experimental test setup records observations using Programmable Logic Controller (PLC) with Supervisory Control and Data Acquisition (SCADA) software. To control the rotational speed of pump, the variable frequency drive (VFD) is connected to an electric motor.

Whole test setup facility was equipped calibrated measuring instruments to measure the various parameters. The suction and delivery pressure head were measured using the pressure transmitters (accuracy $\pm 0.065\%$) with operating range of 0 – 780 mm of Hg and (-14.7) – 500 PS respectively. The non-contact type rotary torque sensor (accuracy $\pm 0.25\%$) having measuring range of 0 – 100 N·m was used to measure the required torque (T). The varying Q was measured using the magnetic flow meter of 0-50 lps capacity with an accuracy of $\pm 0.5\%$.

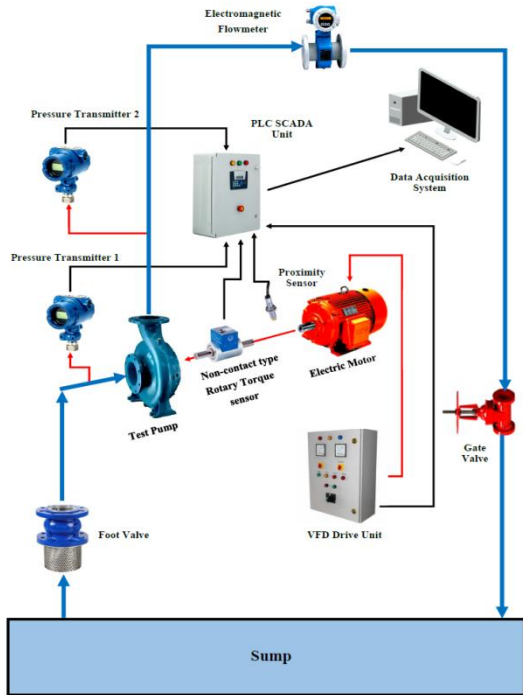


Fig 5. Schematic layout of the test setup.

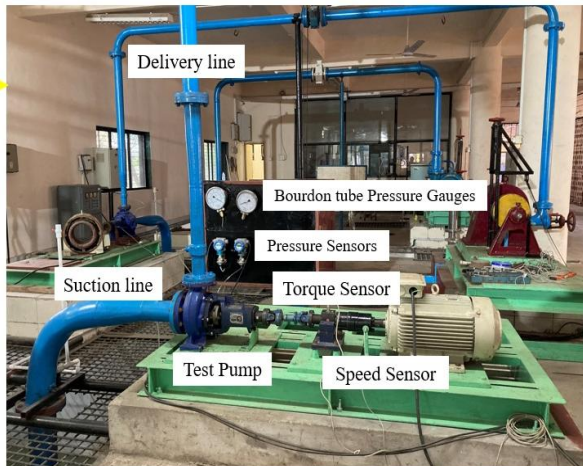


Fig 6. Actual experimental setup established at laboratory.

3. Results and Discussion

In this research analysis, the $N_s = 54$ rpm centrifugal pump was experimented for without and with SCR at rated 1450 and 1000 rpm. For the experimental uncertainty, the experiments were performed total of three times under the same operating conditions at both rpms. The average values of obtained observation were taken into consideration for in-depth analysis. The internal statistical uncertainties were found to be in the range of $\pm 10\%$. The variation in performance characteristic curve parameters, reduction in losses, disk friction coefficient (C_m) and power loss due to disk friction (P_{RR}) were main highlight of the analysis.

Figure 7 and 8, shows the variation in performance characteristic curve parameters at rated 1450 and 1000 rpm. It is derivable from the figures that using SCR at higher Q towards highest efficient point (HEP), the increment in head (ΔH), reduction in required torque (ΔT) and increment in efficiency ($\Delta \eta$) was higher compare to the lower Q . At 1450 rpm and highest efficiency point (HEP), the $\Delta H \uparrow$, $\Delta T \downarrow$ and $\Delta \eta \uparrow$ were 0.0813 m, 0.0561 N·m and 1.7356 % respectively. While the $\Delta H \uparrow$, $\Delta T \downarrow$ and $\Delta \eta \uparrow$ were 0.0593 m, 0.0165 N·m and 1.5592 % at 1000 rpm and HEP. The average observations for various Q are tabulated in Table 1 and 2 for 1450 and 1000 rpm respectively.

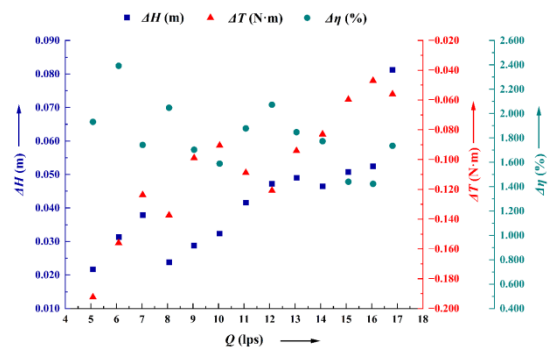


Fig 7. Variation in performance characteristic curve parameters at 1450 rpm.

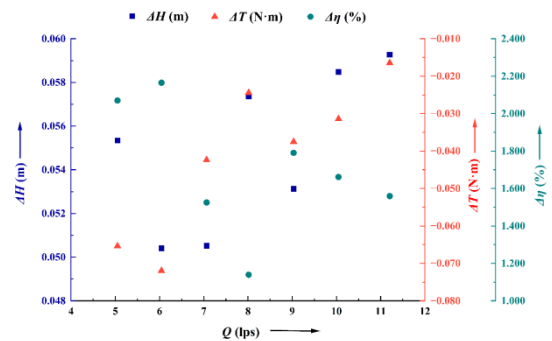


Fig 8. Variation in performance characteristic curve parameters at 1000 rpm

Table 1: Performance characteristic parameters and its variation at 1450 rpm.

Q (lps)	H (m)			T (N·m)			η (%)		
	Without SCR	With SCR	$\Delta H \uparrow$	Without SCR	With SCR	$\Delta T \downarrow$	Without SCR	With SCR	$\Delta \eta \uparrow$
16.812	5.220	5.301	0.081	6.854	6.798	-0.056	82.952	84.688	1.736
16.051	5.372	5.424	0.052	6.714	6.667	-0.047	83.065	84.488	1.423
15.085	5.537	5.587	0.051	6.546	6.486	-0.060	82.228	83.669	1.440
14.074	5.673	5.719	0.047	6.372	6.289	-0.083	80.817	82.590	1.773
13.052	5.732	5.781	0.049	6.197	6.103	-0.094	78.042	79.890	1.848
12.091	5.746	5.793	0.047	5.976	5.856	-0.121	74.921	76.994	2.073
11.067	5.803	5.845	0.042	5.700	5.592	-0.109	72.766	74.644	1.878
10.044	5.868	5.900	0.032	5.412	5.322	-0.091	70.393	71.982	1.589
9.043	5.937	5.966	0.029	5.207	5.109	-0.099	66.709	68.413	1.704
8.064	5.980	6.004	0.024	4.961	4.824	-0.137	62.816	64.863	2.048
7.028	5.985	6.023	0.038	4.655	4.531	-0.124	58.965	60.707	1.743
6.088	6.005	6.037	0.031	4.421	4.265	-0.156	52.893	55.285	2.392
5.081	6.035	6.057	0.022	4.208	4.015	-0.192	47.185	49.117	1.932

Table 2: Performance characteristic parameters and its variation at 1000 rpm.

Q (lps)	H (m)			T (N·m)			η (%)		
	Without SCR	With SCR	$\Delta H \uparrow$	Without SCR	With SCR	$\Delta T \downarrow$	Without SCR	With SCR	$\Delta \eta \uparrow$
11.204	2.519	2.578	0.059	3.267	3.251	-0.017	55.943	57.502	1.559
10.047	2.645	2.704	0.059	3.143	3.111	-0.031	54.800	56.461	1.661
9.033	2.719	2.772	0.053	3.037	3.000	-0.038	52.235	54.026	1.790
8.015	2.727	2.785	0.057	2.848	2.824	-0.024	50.046	51.186	1.139
7.063	2.765	2.816	0.051	2.677	2.635	-0.042	47.192	48.717	1.525
6.044	2.803	2.854	0.050	2.543	2.471	-0.072	43.090	45.254	2.165
5.049	2.810	2.866	0.055	2.331	2.266	-0.065	39.249	41.319	2.070

The improvement in characteristic curve performance parameters using SCR can be explained as: In original pump without SCR the fluid entering the clearance space behaves like a separate external rotating disk which obstructs the free movement of the impeller. This interference increases the starting T requirement to run the pump. Further, there is more H loss due to the unavoidable vortices' formation near the mixing zone. Using SCR reduces the S , which helps in maintaining the uniform flow by diminishing the flow separation. Also, it provides smoother operation of the impeller reducing the input T . Lower the S , lower the enmeshment of fluid and higher the conversion of kinetic energy into pressure energy leading to the increment in H . These efficient enhancement in H and reduction in T ultimately improves the η of pump.

Theoretical head loss with SCR ($(\delta H_l)_{with,SCR}$) and without SCR ($(\delta H_l)_{without,SCR}$) was calculated as below for better understanding of the SCR phenomena and its effect on pump performance:

$$\begin{aligned}
 & (\delta H_l)_{with,SCR \text{ or } without,SCR} \\
 & = (H_{max})_{with,SCR \text{ or } without,SCR} \\
 & \quad - (H)_{with,SCR \text{ or } without,SCR}
 \end{aligned} \tag{1}$$

where,

$$\begin{aligned}
 & (H_{max})_{with,SCR \text{ or } without,SCR} \\
 & = \frac{(T)_{with,SCR \text{ or } without,SCR} \times \omega}{\rho g Q}
 \end{aligned} \tag{2}$$

The calculated δH_l for 1450 rpm and 1000 rpm at various Q was graphically represented in Figure 9 and 10 respectively. It is but obvious that $(\delta H_l)_{with,SCR}$ is always less than $(\delta H_l)_{without,SCR}$ at all Q . Further, at lower Q difference in δH_l is higher and it reduces towards the higher Q . The average $(\delta H_l)_{with,SCR}$ of 2.52 m and $(\delta H_l)_{without,SCR}$ of 2.75 m was obtained for 1450 rpm, while $(\delta H_l)_{with,SCR}$ of 2.94 m and $(\delta H_l)_{without,SCR}$ of 2.79 m was obtained for 1000 rpm. This reduction in δH_l is best indication of the improvement in pump performance using SCR in pump.

Because the cylindrical SCR better seals the space between the impeller and the volute, it probably

provides a more effective barrier against fluid recirculation.

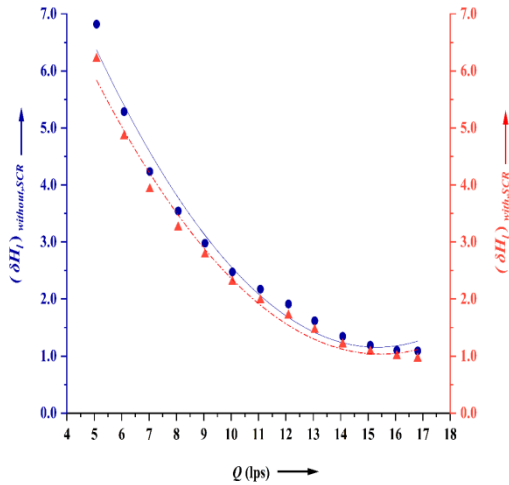


Fig9. Theoretical δH_l at 1450 rpm.

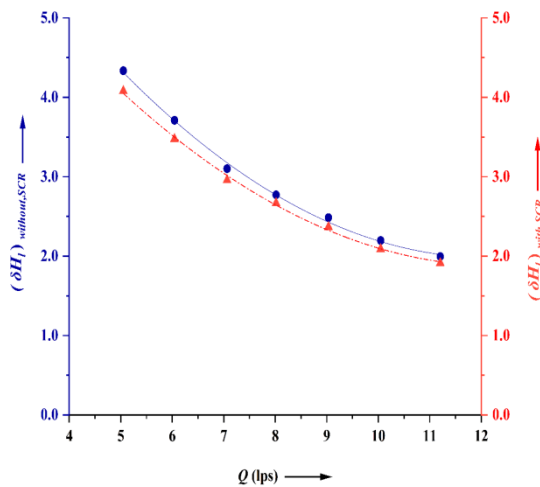


Fig 10: Theoretical δH_l at 1000 rpm.

This design may minimize the chance of high-pressure fluid leaking back into the low-pressure area by providing a more uniform and wider surface area in contact with the fluid. Moreover, the cylindrical SCR may minimize turbulence and energy losses by offering a more steady and uniform flow pattern. As a result, the fluid is better trapped inside the intended flow path, transferring more of the impeller's energy to the fluid and improving the pump's overall performance.

For further investigation and clarification, C_m and P_{RR} were calculated using various empirical relations provided by the various researchers as stated in Table 3.

Table 3: Correlation for C_m and P_{RR} by various researchers.

Reference	Correlation for C_m and P_{RR}
Gülich[22]	$C_m = \frac{0.0255}{R_e^{0.2}} (S^*)^{0.1}, S^* = \frac{S}{R}, R_e = \frac{\omega R^2}{\vartheta}$ (3)
	$P_{RR} = \frac{C_m}{\cos \delta} \rho \omega^3 R^5 \left(1 - \left(\frac{R_i}{R}\right)^2\right)$ (4)
Poullikkas et al. [23]	$C_m = \left(\frac{k}{R}\right)^{0.25} \times \left(\frac{S}{R}\right)^{0.1} \times R_e^{-0.2}$ (5)
	$P_{RR} = C_m \rho \omega^3 R^5$ (6)
Daily and Nece[24]	$C_m = \frac{0.0102(S/R)^{1/10}}{R_e^{1/5}}$ (7)
	$P_{RR} = C_m \rho \omega^3 R^5$ (8)
Pfleiderer and Petermann[25]	$C_m = 7.3 \times 10^{-4} \times \left(\frac{2 \times \vartheta \times 10^6}{u \times D}\right)^{1/8}$ (9)
	$P_{RR} = C_m \times \rho \times (u)^3 \times D(D + 5S)$ (10)

Where, R_e is Reynolds number, R is radius of impeller in m, ω is angular velocity in rad/s, ϑ is kinematic viscosity in m^2/s , δ is blade angle, ρ is density in kg/m^3 , k is surface roughness in μm , u is velocity in m/s and D is diameter of impeller in m. Figure 11 and 12 represents the variation of C_m along the S from 13 mm to 1 mm for 1450 and 1000 rpm respectively. As seen from the Figs. varying the S from 13 mm to 1 mm will reduce the C_m . This variation is similar for all the empirical relations provided by the various researchers as per Table 3, except for the relation given by Pfleiderer and Petermann [25]. Similarly, the variation of P_{RR} along the S for 1450 and 1000 rpm is depicted in Fig. 13 and 14 respectively.

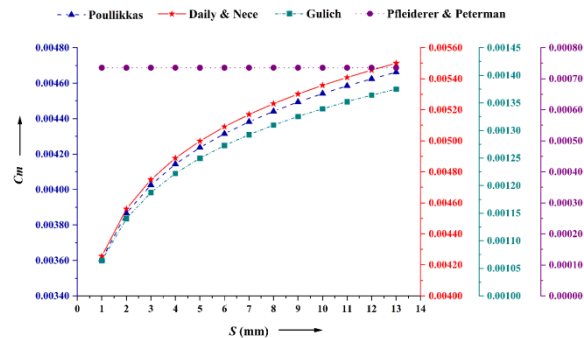


Fig 11. C_m vs S at 1450 rpm.

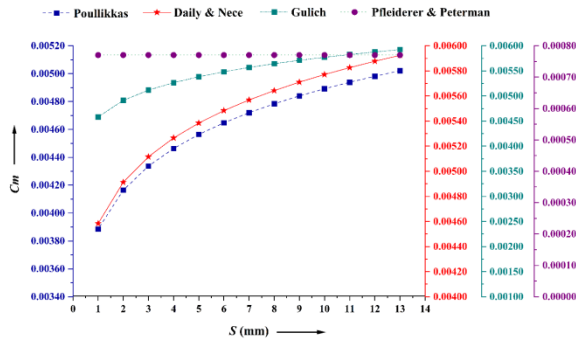


Fig 12. C_m vs S at 1000 rpm.

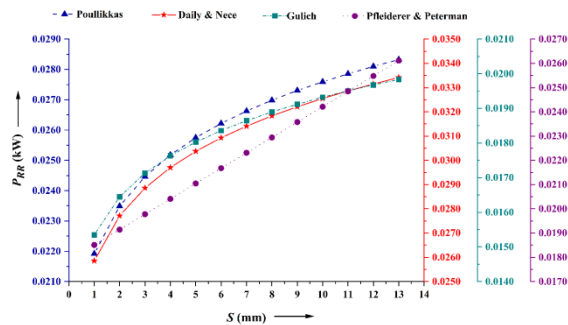


Fig 13. P_{RR} vs S at 1450 rpm.

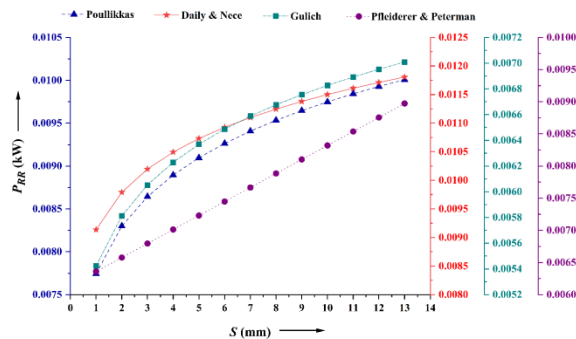


Fig 14. P_{RR} vs S at 1000 rpm.

4. Conclusion

In the current article centrifugal pump without and with SCR was studied experimentally to check the performance of $N_s - 54$ rpm centrifugal pump. The experiments were examined on well-established and calibrated ring at Fluid Mechanics and Fluid Machine Laboratory, SardarVallabhbai National Institute of Technology, Surat, Gujarat, India. Using SCR, the pump performance improves notably. The important findings of the research are:

By lowering the S and hence lowering the DF_l , SCR installation improves the centrifugal pump performance. By preventing the fluid from accessing the back-side clearance zone, SCR prevents the formation of a core flow in the S and preserves a

more consistent flow pattern in the volute. Further, the efficient conversion of kinetic energy into pressure energy SCR increases ΔH , reduces ΔT and enhances overall $\Delta \eta$ at both 1450 and 1000 rpm. Also, theoretical δH_l at without and with SCR conditions as well as C_m and P_{RR} supports the obtained betterment in performance of pump.

Although, this study provides the robust foundation for improvising the pump performance, other practical design modification needs to be studied. Further, the actual implementation in already installed various kind of pumps in industries needs to be explored.

Acknowledgments

The authors sincerely acknowledge the support from SardarVallabhbai National Institute of Technology, Surat and Sarvajani College of Engineering & Technology, Surat. The authors are also thankful to Mr. Sivadasan, Mr. Pruthviraj Solanki, and Mayank Patel for their contribution toward the development of test rig and experimental work.

References

- [1] P. Waide and C. U. Brunner, "Energy-Efficiency Policy Opportunities for Electric Motor-Driven Systems. International Energy Agency," *Energy Effic. Ser.*, p. 132, 2011.
- [2] V. K. Arun Shankar, S. Umashankar, S. Paramasivam, and N. Hanigovszki, "A comprehensive review on energy efficiency enhancement initiatives in centrifugal pumping system," 2016. doi: 10.1016/j.apenergy.2016.08.070.
- [3] J. M. Fernández Oro, R. Barrio Perotti, M. Galdo Vega, and J. González, "Effect of the radial gap size on the deterministic flow in a centrifugal pump due to impeller-tongue interactions," *Energy*, vol. 278, 2023, doi: 10.1016/j.energy.2023.127820.
- [4] S. Oshurbekov, V. Kazakbaev, V. Prakht, V. Dmitrievskii, and L. Gevorgov, "Energy consumption comparison of a single variable-speed pump and a system of two pumps: Variable-speed and fixed-speed," *Appl. Sci.*, vol. 10, no. 24, pp. 1–14, 2020, doi: 10.3390/app10248820.
- [5] T. Capurso, L. Bergamini, and M. Torresi, "A new generation of centrifugal pumps for high conversion efficiency," *Energy Convers. Manag.*, vol. 256, 2022, doi: 10.1016/j.enconman.2022.115341.
- [6] A. Doshi, S. Channiwalla, and P. Singh, "Influence of Nonflow Zone (Back Cavity)

- Geometry on the Performance of Pumps as Turbines,” *J. Fluids Eng. Trans. ASME*, vol. 140, no. 12, 2018, doi: 10.1115/1.4040300.
- [7] K. A. Kaupert and T. Staubli, “The unsteady pressure field in a high specific speed centrifugal pump impeller—Part I: Influence of the volute,” *J. Fluids Eng. Trans. ASME*, vol. 121, no. 3, pp. 621–626, 1999, doi: 10.1115/1.2823514.
- [8] N. Pedersen, P. S. Larsen, and C. B. Jacobsen, “Flow in a centrifugal pump impeller at design and off-design conditions - Part I: Particle image velocimetry (PIV) and laser Doppler velocimetry (LDV) measurements,” *J. Fluids Eng. Trans. ASME*, vol. 125, no. 1, pp. 61–72, 2003, doi: 10.1115/1.1524585.
- [9] J. González and C. Santolaria, “Unsteady flow structure and global variables in a centrifugal pump,” *J. Fluids Eng. Trans. ASME*, vol. 128, no. 5, pp. 937–946, 2006, doi: 10.1115/1.2234782.
- [10] H. Liu, K. Wang, S. Yuan, M. Tan, Y. Wang, and L. Dong, “Multicondition optimization and experimental measurements of a double-blade centrifugal pump impeller,” *J. Fluids Eng. Trans. ASME*, vol. 135, no. 1, 2013, doi: 10.1115/1.4023077.
- [11] H. Stel, G. D. L. Amaral, C. O. R. Negrão, S. Chiva, V. Estevam, and R. E. M. Morales, “Numerical analysis of the fluid flow in the first stage of a two-stage centrifugal pump with a vaned diffuser,” *J. Fluids Eng. Trans. ASME*, vol. 135, no. 7, 2013, doi: 10.1115/1.4023956.
- [12] Z. Gao, W. Zhu, L. Lu, J. Deng, J. Zhang, and F. Wuang, “Numerical and experimental study of unsteady flow in a large centrifugal pump with stay vanes,” *J. Fluids Eng. Trans. ASME*, vol. 136, no. 7, 2014, doi: 10.1115/1.4026477.
- [13] C. Wu, K. Pu, C. Li, P. Wu, B. Huang, and D. Wu, “Blade redesign based on secondary flow suppression to improve energy efficiency of a centrifugal pump,” *Energy*, vol. 246, 2022, doi: 10.1016/j.energy.2022.123394.
- [14] Y. Lin, X. Li, Z. Zhu, X. Wang, T. Lin, and H. Cao, “An Energy Consumption Improvement Method for Centrifugal Pump Based on Bionic Optimization of Blade Trailing Edge,” *SSRN Electron. J.*, 2021, doi: 10.2139/ssrn.3972241.
- [15] H. Bozorgasareh, J. Khaledi, M. Jafari, and H. O. Gazori, “Performance improvement of mixed-flow centrifugal pumps with new impeller shrouds: Numerical and experimental investigations,” *Renew. Energy*, vol. 163, pp. 635–648, 2021, doi: 10.1016/j.renene.2020.08.104.
- [16] H. Ding, Z. Li, X. Gong, and M. Li, “The influence of blade outlet angle on the performance of centrifugal pump with high specific speed,” *Vacuum*, vol. 159, pp. 239–246, 2019, doi: 10.1016/j.vacuum.2018.10.049.
- [17] A. F. Ayad, H. M. Abdalla, and A. A. El-Azm Aly, “Effect of semi-open impeller side clearance on the centrifugal pump performance using CFD,” *Aerosp. Sci. Technol.*, vol. 47, pp. 247–255, 2015, doi: 10.1016/j.ast.2015.09.033.
- [18] L. Cao, Y. Zhang, Z. Wang, Y. Xiao, and R. Liu, “Effect of Axial Clearance on the Efficiency of a Shrouded Centrifugal Pump,” *J. Fluids Eng. Trans. ASME*, vol. 137, no. 7, 2015, doi: 10.1115/1.4029761.
- [19] H. Pehlivan and Z. Parlak, “Investigation of parameters affecting axial load in an end suction centrifugal pump by numerical analysis,” *J. Appl. Fluid Mech.*, vol. 12, no. 5, pp. 1615–1627, 2019, doi: 10.29252/JAFM.12.05.29623.
- [20] B. Kim, M. H. Siddique, S. A. I. Bellary, A. S. aljehani, S. W. Choi, and D. E. Lee, “Investigation of a centrifugal pump for energy loss due to clearance thickness while pumping different viscosity oils,” *Results Eng.*, vol. 18, 2023, doi: 10.1016/j.rineng.2023.101038.
- [21] S. Maeda, T. Sano, K. Miyagawa, and K. Sakai, “Reduction of Disk Friction Loss by Applying a Fin to the Back of a Centrifugal Impeller,” *J. Fluids Eng. Trans. ASME*, vol. 146, no. 7, 2024, doi: 10.1115/1.4065047.
- [22] J. F. GÜlich, *Centrifugal pumps, fourth edition*. Springer International Publishing, 2019. doi: 10.1007/978-3-030-14788-4.
- [23] A. Poulikkas, “Surface roughness effects on induced flow and frictional resistance of enclosed rotating disks,” *J. Fluids Eng. Trans. ASME*, vol. 117, no. 3, pp. 526–528, 1995, doi: 10.1115/1.2817294.
- [24] J. W. Daily and R. E. Nece, “Chamber dimension effects on induced flow and frictional resistance of enclosed rotating disks,” *J. Fluids Eng. Trans. ASME*, vol. 82, no. 1, pp. 217–230, 1960, doi: 10.1115/1.3662532.
- [25] H. P. Carl Pfeleiderer, *Strömungsmaschinen*. 2005. doi: 10.1007/b138287.